Plasma edge biasing on CASTOR tokamak using LHCD *)

F. Žáček, V. Petržílka, K. Jakubka, J. Stöckel

Association Euratom/IPP.CR, Za Slovankou 3, 182 21 Prague 8, Czech Republic

J. Gunn, M. Goniche, P. Devynck

Association Euratom/CEA, Cadarache, France

M. Podesta

CESNEF, Politecnico di Milano, Italy

S. Nanobashvili

Institute of Physics, Tamarashvili 6, 380077 Tbilisi, Georgia

Received 1 October 2001

The interaction of high power lower hybrid waves with tokamak plasma results in a range of favourable but also unfavourable effects. This article deals with the effects observed by Langmuir probes on the small tokamak CASTOR. The most pronounced effects found are positive biasing of the whole plasma periphery and the formation of a negative "well" of floating potential in front of the launcher.

1 Introduction

High power Lower Hybrid Waves (LHW) are used commonly in tokamaks for non-inductive current drive (LHCD) with the aim to control the electrical current profile and in this way to achieve an improvement of the plasma confinement or even to achieve a stationary tokamak operation without the necessity to use any transformer.

Besides dragging fast electrons carrying the electrical current, several other phenomena resulting from LHW–plasma interaction are observed in many tokamaks. Some of these phenomena, like formation of a steeper edge potential gradient (edge "biasing" [1]), are probably resulting in improvement of global plasma parameters, while others can lead to the deterioration of the discharge properties by the undesirable generation of fast superthermal particles just in front of the launcher [2], followed by potential damages of those plasma facing components connected directly with the interaction region by magnetic field lines [3].

This article deals with accompanying effects observed with LHCD in the plasma of the tokamak CASTOR. The main attention is concentrated on the measurements of changes in the edge plasma potential. The structure of the article is the following. Section 2 describes the experimental arrangement concerning LH launching system

*) Presented at the 4th Europhysics Workshop "Role of Electric Fields in Plasma Confinement and Exhaust", Funchal, Madeira, Portugal, June 24–25, 2001

as well as diagnostics used. The effects observed in CASTOR can be divided into two groups. Section 3 describes therefore the "macroscopic" effects observable in the whole periphery of the tokamak (and resulting probably in the changes of total plasma characteristics as is e.g. improvement of particle confinement [4]), while Sect. 4 describes the effects occurring only in the region close to the CASTOR launching antenna [5]. Section 5 summarises the results and conclusions.

2 Experimental arrangement

CASTOR is a small limiter tokamak with major radius $R = 0.4\,\mathrm{m}$, wall radius $b = 0.1\,\mathrm{m}$ and limiter radius $a = 0.085\,\mathrm{m}$. Magnetic field on the device axis $B(0) \leq 1.5\,\mathrm{T}$ (supplied by a condenser bank $0.32\,\mathrm{F}$ with energy up to $1\,\mathrm{MJ}$), plasma density in the centre $n(0) \leq 3 \times 10^{19}\mathrm{m}^{-3}$ and length of the discharge $\tau \leq 40\,\mathrm{ms}$ with the current up to $20\,\mathrm{kA}$.

For the LH experiments in CASTOR a three-waveguide multijunction grill working at the frequency $f = 1.25\,\mathrm{GHz}$ and power up to $50\,\mathrm{kW}$ is used. Output dimensions of the grill mouth are $160\,\mathrm{mm}$ in the poloidal and $50\,\mathrm{mm}$ in the toroidal directions. The grill is partially shaped in the poloidal plane to follow the magnetic surface at the radius $r = 86\,\mathrm{mm}$ (see also Fig. 2 on the next page). A typical discharge in the CASTOR LHCD regime is shown in Fig. 1, where the loop voltage U_{loop}, plasma current I_{p}, line averaged density $\bar{n}$ (measured by a $4\,\mathrm{mm}$ microwave interferometer) and LHW incident power P_{LH} are given. The lowest trace is the value of the non-inductive current I_{LH} driven by LHW (evaluated from the relative drop of U_{loop}). It may be seen that 60% of the total current is driven by LHW during the RF pulse at the density $\bar{n} = 4 \times 10^{18}\mathrm{m}^{-3}$ (efficiency of the current

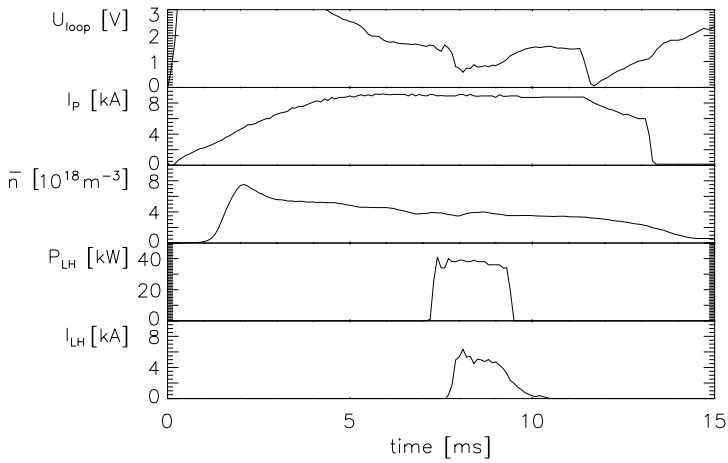

Fig. 1. Loop voltage U_{loop}, plasma current I_{p}, line averaged density $\bar{n}$, incident LH power P_{LH} and noninductively generated LH current I_{LH} in a typical CASTOR discharge with LHCD (shot #5581).

drive is decreasing with the increasing plasma density and it is going to zero in CASTOR, due to relatively low LHW frequency used, if plasma density approaches value $\bar{n} \simeq 10^{19}\mathrm{m}^{-3}$).

For the measurements of changes of peripheral plasma floating potential V_{fl} in CASTOR due to the LHW application, several different Langmuir probe systems have been used:

(i) Radial rake of 16 probes with equal spacing 2.5 mm (placed 180° or 135° toroidally away from the grill from the top or from the low field side in the equatorial plane) for measurement of time development of radial profiles during one shot.

(ii) Double probe with poloidally separated tips (placed in tokamak equatorial plane 180° or 135° toroidally away from the grill) for the determination of the poloidal rotation velocity of plasma fluctuations using a two-point correlation technique.

(iii) A single probe rotating fast in the poloidal plane to determine radial profiles of the floating potential during a single shot, placed 135° toroidally away from the grill in horizontal diagnostics port (radius of the probe rotation is 30 mm and depth of the radial penetration into the plasma about 20 mm, see Fig. 5 below, the time of one profile measurement about 1 ms).

(iv) A special double coaxial probe with tips spaced toroidally by 3.5 mm (diameter 0.5 mm, length 1.5 mm) for measurements of radial profiles of floating potential V_{fl} just in front of the grill (or even inside the waveguides) [5]. The probe is fixed in a spherical joint located about 500 mm above the centre of the tokamak small cross section where the grill is placed. This arrangement enabled us to change the radial as well as the toroidal position of the measuring tips on the shot-to-shot basis (by a tilting of the probe), see Fig. 2. Further, vertical shift of the probe along its axis enables to change the position of the tips also in the third dimension, denoted in Fig. 2 as h (height above the equatorial plane of the torus).

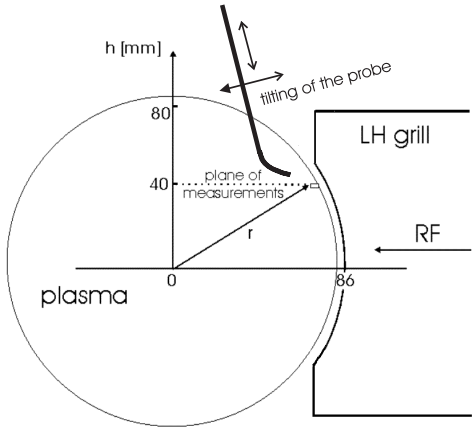

Fig. 2. Schematic of CASTOR small cross-section with the lower hybrid grill (radius of the grill circular shaping 86 mm, aperture limiter radius 85 mm).

3 Probe measurements in the region far from the LHW launcher

The most general feature observed during the LHCD in CASTOR is an increase of the plasma floating potential, i.e. a positive biasing of the peripheral plasma. This biasing is detectable in the periphery of the whole tokamak. Figures 3a,b show two examples obtained using the radial rake of 16 probes placed in tokamak from the top of the device at the toroidal position 180° away from the grill. Three time averaged profiles of floating potential are shown in these figures: one in ohmic regime (just before the RF application) — triangles, connected by the full line and two in two subsequent time periods (differing by 1 ms) during RF — asterisks and diamonds. Figure 3a has been measured in the case with a relatively low averaged density $\bar{n} \approx 4 \times 10^{18}\mathrm{m}^{-3}$ (i.e. in the case with high percentage of noninductively generated current corresponding to the Fig. 1), the Fig. 3b in the case with higher density $\bar{n} \approx 10 \times 10^{18}\mathrm{m}^{-3}$ (with hardly any observable LH current drive). A well expressed connection between the effect of positive plasma "biasing" and current drive efficiency can be seen when the two figures are compared.

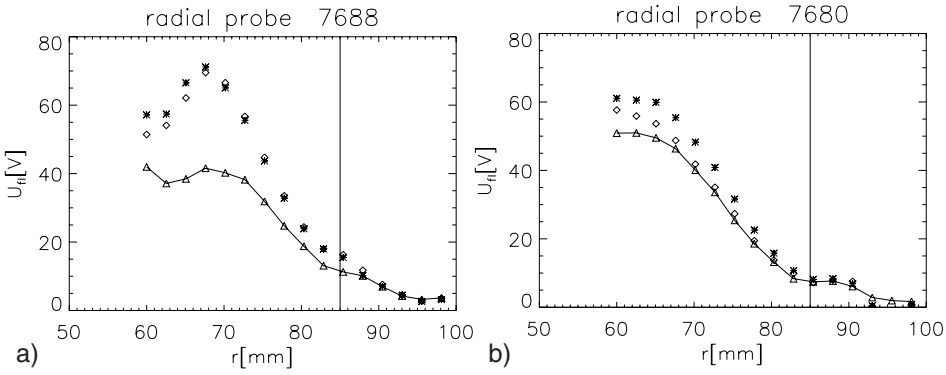

Fig. 3. Radial profiles of the probe floating potential during *ohmic* (triangles connected by a full line) and RF (in two times differing by 1 ms — diamonds and asterisks) regimes, measured by a radial rake of 16 probes inserted in the tokamak from the top at the toroidal position 180° away from the grill. The values of the floating potential given in the figure are averaged over 10^3 samples (i.e. over period 1 ms); left side — shot #7687 with averaged plasma density $\bar{n} \approx 4 \times 10^{18}\mathrm{m}^{-3}$; right side — #7680 with averaged plasma density $\bar{n} \approx 10 \times 10^{18}\mathrm{m}^{-3}$.

Another interesting manifestation of LHCD, observed in CASTOR during earlier measurements [4] and using another probe technique, can be seen in Fig. 4. In this figure time developments of the poloidal velocity v_p of the floating potential fluctuations are given. The values of v_p have been evaluated by two-point correlation technique on shot-to-shot basis from data registered by the double poloidal probe (mentioned in Sect. 2, point (ii)), located on several different radii ($r = 82$, 84 and 86 mm). An increase of this velocity can be seen starting from the moment of LHCD application ($t = 15$ ms on curves denoted as LH in the figure). Moreover, an

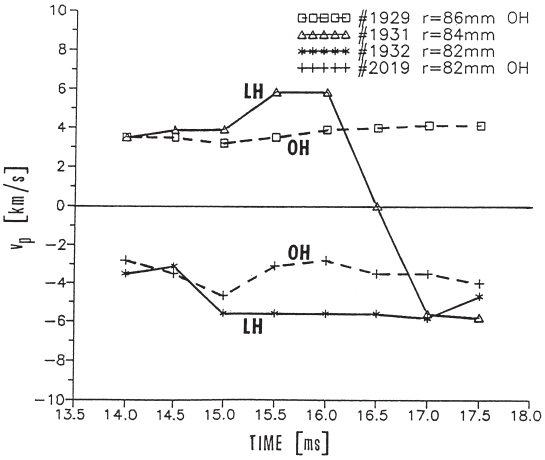

Fig. 4. Time evolution of poloidal velocity v_p at three different radii of double poloidal probe ($r = 82$, 84 and 86 mm) in OH and LHCD regimes (poloidal separation of the probes 7 mm); positive sign of v_p (in outer part of the periphery) has direction of the electron diamagnetic drift velocity.

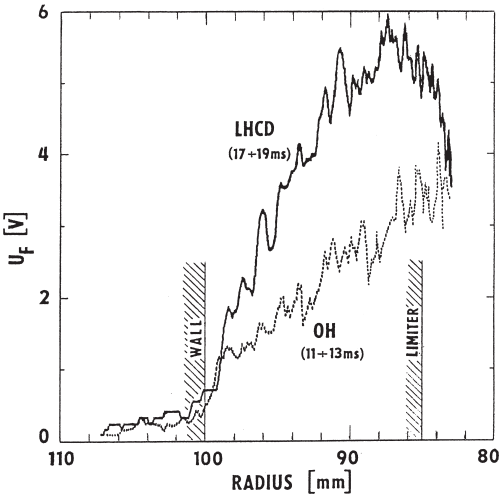

Fig. 5. Comparison of radial profiles of the plasma floating potential in OH and LHCD regimes (measured by rotating probe).

outward directed radial shift of poloidal velocity shear layer (the layer with radius on which the poloidal rotation changes its sign) is observed during the LHW application (see transition of this layer after application of LHW power over the probe if the probe is located on the radius $r = 84\,\mathrm{mm}$). Figure 5 shows the comparison of the radial distribution of the floating potential (i.e. also radial electric field) before and during LHCD. This measurement has been done by rotating probe penetrating into the plasma from horizontal port (see point (iii) in Sect. 2). Note that during its radial penetration this probe changes also its poloidal position (by about 15°). The Fig. 5 proves that observed increase of velocity of poloidal rotation as well as radial shift of the velocity shear layer is caused by LHW positive plasma "biasing" (i.e. by the change of the radial electric field profile). Let us note that theory explains such positive plasma biasing by enhanced generation (and also escape) of the runaway electrons [1].

4 Probe measurements in front of the CASTOR launcher

Because of a high LHW power used, the wave-plasma interaction can be accompanied by a number of non-linear effects, especially in the region near to the launcher [2,3].

To verify the predictions of theory concerning acceleration of the fast particles just in front of the launcher, measurements have been done on CASTOR using the movable Langmuir probe mentioned in Sect. 2, point (iv). The probe position has been changed from shot to shot and due to the high reproducibility of the CASTOR discharges a detailed map of the floating potential in front of the grill has been established during several hundreds of shots.

Figure 6 shows a 3D picture of the situation in a horizontal plane with $h = 40\,\mathrm{mm}$ (see Fig. 2) when LHW is applied, obtained by a detailed radial scan (1 mm or even smaller step) of the probe in five different toroidal positions z denoted in the figure as A, B, C, D and E (see these positions relative to the grill waveguides walls, depicted in the figure by thick lines). As the most striking phenomenon, formation of a radially very narrow layer (several mm only) of the plasma floating potential drop (negative potential "well") can be seen in the figure. To see the formation and radial extent of the potential "well" in more detail, Fig. 7 shows the comparison of a radial cut of Fig. 6 just in the centre of the grill (i.e. $z = 0\,\mathrm{mm}$) with the case of zero LHW power. In addition to the formation of a deep negative potential "well" (over 100 V in this case) in a narrow radial layer, the positive biasing of the edge plasma on both sides of this layer can be seen in Fig. 7 as well when LHW is applied. It means that the effect of the positive "biasing" discussed in the foregoing Sect. 3 is also observed in front of the launcher, while the formation of a radially narrow negative potential "well" is only observed in front of the grill.

The latter fact is demonstrated below by poloidal (Fig. 8) and toroidal (Fig. 9) dependencies of the maximum floating potential drop (found by the radial scan of the probe position). It may be seen from Fig. 8 that the depth of the potential "well" (triangles, full line) decreases in poloidal direction (i.e. along the longer

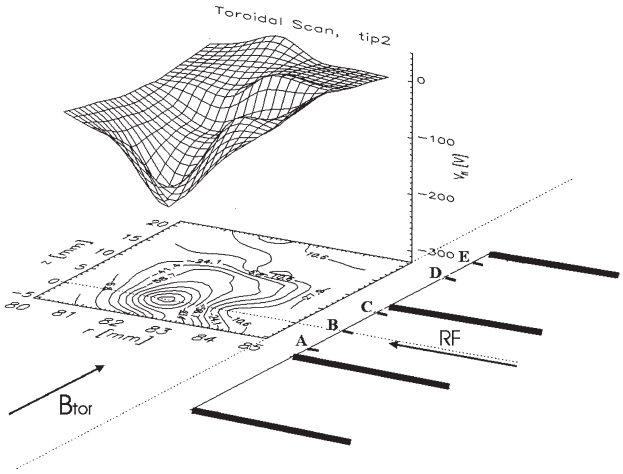

Fig. 6. Toroidal versus radial plot of the floating plasma potential in front of the CASTOR grill (averaged over 1 ms period) under LHW application, obtained by a radial scan of the probe in five different toroidal positions A,B,C,D, and E at the horizontal plane $h = 40$ mm.

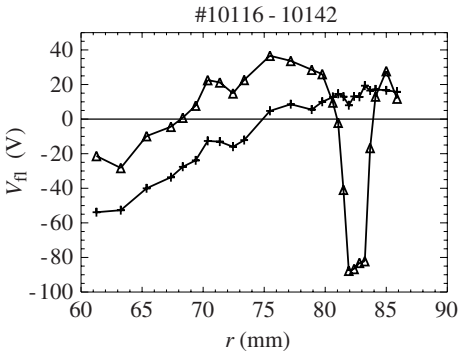

Fig. 7. Radial profiles of the probe floating potential measured by movable probe in the centre of the grill (i.e., $z = 0$ mm) at $h = 40$ mm; crosses — without LHW, triangles — LHW applied.

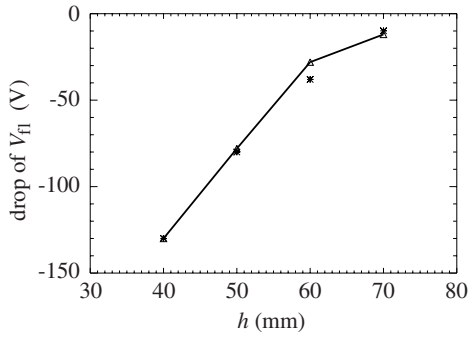

Fig. 8. Comparison of the measured radial maximum of V_{fl} drop (triangles — full line) with squared value (normalized at $h = 40$ mm) of the electric field intensity in waveguide (asterisks), in dependence on the vertical probe position h (vertical dimension of the grill is ± 80 mm).

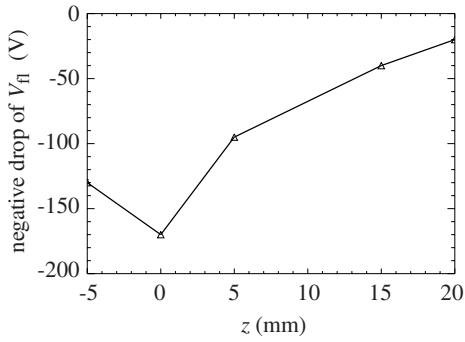

Fig. 9. Toroidal dependence of the maximum V_{fl} drop measured at the horizontal plane $h = 40\,\mathrm{mm}$.

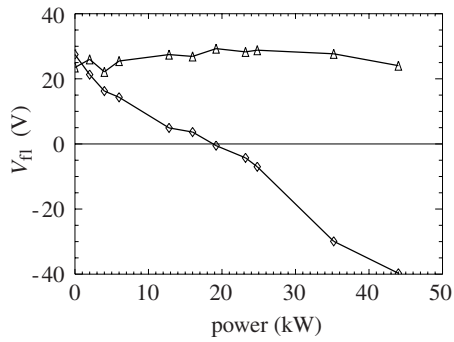

Fig. 10. Dependence of the probe floating potential V_{fl} measured during LHW pulse on LHW power — diamonds (probe location $z = 0\,\mathrm{mm}$, $h = 60\,\mathrm{mm}$) ; for comparison, V_{fl} in *ohmic* regime just before LHW application — triangles.

wall of the waveguides) from the centre in accordance with the square of sinusoidal distribution of the electric field in the grill waveguides (asterisks). Fig. 9 shows that similar dependence of the floating potential drop has been found also in the toroidal direction, i.e. the maximum depth of the potential "well" seems to be located in front of the launcher centre.

Dependence of the floating potential drop on the power used in CASTOR is shown in Fig. 10 (probe position $z = 0\,\mathrm{mm}$, $h = 60\,\mathrm{mm}$). Linear proportionality without any threshold effect may be seen quite well from the figure.

Because the drop of floating potential in such a narrow layer is most probably the result of fast electrons generated in this layer, an attempt to prove the existence of such electrons by analysis of the probe I–V characteristics (measured just in the place of the "well" location) has been done, see Fig. 11 (1 kHz sinusoidal voltage has been used for the sweeping). However, fitting of the electron temperature to the characteristics indicates an increase of the bulk electron temperature rather than the existence of some measurable group of accelerated electrons. It may be seen from the figure that if such electrons exist, their contribution is quite overlapped by non-saturation effect of the ion current observed with increasing (negative) probe voltage in the OH regime, too.

5 Discussion of results and summary

During the LHCD experiments on tokamak CASTOR a whole range of interesting physical phenomena is observed. Because CASTOR is very well equipped with different kinds of Langmuir probe diagnostics, most effects reported in this article have been detected by Langmuir probes in the plasma periphery of the whole tokamak torus. Nevertheless, to better see the close link between periphery and

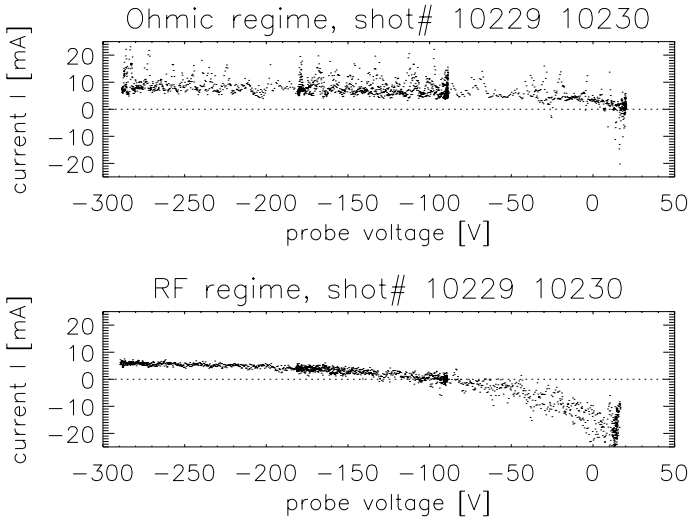

Fig. 11. Example of I–V characteristics measured during LHW application at the radius of the maximum V_{fl} drop; upper trace — without LHW, lower trace — LHW applied (note the shift of V_{fl} by about $-100\,\mathrm{V}$).

plasma core, in the following we also summarize changes in some global plasma characteristics described already elsewhere (see e.g. [4,6]), because these changes are resulting unambiguously just from the effects observed in the plasma periphery.

The main results of our measurements on CASTOR can be summarized as follows:

(i) increase of plasma floating potential up to several tens of volts (i.e. positive "biasing") of the plasma periphery is registered everywhere along the plasma torus in regimes with an observable current drive effect;

(ii) according to the theory [1] this effect of positive plasma biasing during LHCD can be attributed to enhanced production of runaway electrons (and in a quasistationary state also to enhanced non-ambipolar losses of these electrons resulting just in observed biasing during LHCD);

(iii) radial electric field enhanced in such a way results in an increase of poloidal plasma rotation;

(iv) in addition, outward shift of poloidal velocity shear layer during LHCD is registered in the whole plasma periphery;

(v) as accompanying effect a reduction of electrostatic as well as magnetic fluctuations [4], steepening of density gradient in the periphery region [6] and generally increase of the global particle confinement time are observed in CASTOR [4];

(vi) formation of a radially very narrow (only several mm) layer with an expressive floating potential drop (a negative potential "well") has been found close to the grill mouth when LHW is applied [5];

(vii) depth of this "well" depends linearly on LH power and it may probably reach a value of several hundreds volts in front of the centre ($z = 0$ mm, $h = 0$ mm) of the CASTOR launcher;

(viii) the depth of this potential "well" decreases in poloidal as well as in toroidal directions from the centre of the grill;

(ix) formation of this "well" could indicate existence of the fast electrons generated in this layer by the launched LH wave;

(x) however, an attempt to find such fast electrons by analysis of the probe I–V characteristics, measured just in radial position of the "well", did not bring the expected results up to now; to find an adequate answer to this question, measurements of particle distribution function using a retarding field analyser are under preparation.

The work has been supported by the Grant GA AV CR 1043101 and by the Project Barrande 2000-1.

References

[1] I. Voitsekhovich, J. Stöckel, and F. Žáček: in *Proc. 20th EPS Conf. on Contr. Fusion and Plasma Phys.*, Lisbon 1993 (Eds. J.A. Costa Cabral, M.E. Manso, F.M. Serra, and F.C. Schüller), EPS, Geneve, 1993, Pt. I, p. 151.

[2] V. Petržílka, K. Jakubka, R. Klíma, L. Krlín, P. Pavlo, J. Stöckel, F. Žáček, D. Tskhakaya, S. Kuhn, J.A. Tataronis, V. Fuchs, and M. Groniche: Czech. J. Phys. **49**/Suppl. S3 (1999) 127.

[3] V. Petržílka, F. Žáček, B. Kolman, F. Kroupa, K. Jakubka, J. Stöckel, R. Klíma, L. Krlín, and P. Pavlo: in *Proc 18th IAEA Fusion Energy Conference*, Sorrento, Italy, October 2000, paper EXP 4/07.

[4] F. Žáček et al.: *Proc. 18th EPS Conf. on Contr. Fus. and Plasma Physics*, Berlin 1991 (Eds. P. Bachman and D.C. Robinson), EPS, Geneve, 1991, Pt. III, p. 341.

[5] F. Žáček et al.: in *Proc. 28th EPS Conf. on Contr. Fusion and Plasma Phys.*, Funchal 2001, poster 276, in print.

[6] F. Žáček, K. Jakubka, J. Badalec, J. Stöckel, Kletečka P. , L. Kryška, and V. Kříha: Czech. J. Phys. **44** (1994) 121.